Dependence of run-up on coastal bathymetry

ISSN 1870-9095

Supriya Chatterjee
Department of Physics, Bidhannagar College, EB – 2, Sector – 1, Salt Lake, Kolkata, 700064, India.

E-mail: supriya_2k1@rediffmail.com

(Received 10 October 2022, accepted 29 November 2022)

Abstract

We propose a general model of coastal bathymetry for estimating the run-up on it during tsunami. The model for bathymetry is considered as $h(x) = -\alpha x^n$, where α is termed as the steepness parameter and n determines the shape of bathymetry. A linear differential equation has been derived from the shallow water equations of Euler in one-dimension. An analytical solution of the equation is obtained. We find that as n increases the run-up of tsunami in the coastal region also increases for fixed α. On the other hand, the run-up also increases as α increase for a particular n. It is established that the waves with lower frequency (higher time period) produce larger run-up.

Keywords: Tsunami, run-up, coastal bathymetry.

Resumen

Proponemos un modelo general de batimetría costera para estimar el run-up sobre la misma durante un tsunami. El modelo de batimetría se considera como $h(x) = -\alpha x^n$, donde α se denomina parámetro de pendiente y n determina la forma de la batimetría. Se ha derivado una ecuación diferencial lineal a partir de las ecuaciones de aguas poco profundas de Euler en una dimensión. Se obtiene una solución analítica de la ecuación. Encontramos que a medida que n aumenta, la aceleración del tsunami en la región costera también aumenta para α fijo. Por otro lado, el run-up también aumenta a medida que aumenta α para un n particular. Se establece que las olas de menor frecuencia (mayor período de tiempo) producen mayor run-up.

Palabras clave: Tsunami, run-up, batimetría costera.

I. INTRODUCTION

Tsunamis cause devastation in the coastal area due to run-up and inundation and the various aspects of tsunami are interesting fields of research [1]. Tsunamis are usually caused by underwater earthquakes. In addition to this, volcanic eruptions, landslides, large meteorite impact also have the potential to generate a tsunami [2]. In the subduction zone where an oceanic plate of relatively higher density suddenly goes below the continental plate of lower density may cause the centre of tsunami and from this place a series of waves that rush outwards – the beginning of tsunami [3]. These waves travel very far and very fast. The velocity of tsunami is $c=\sqrt{(gH)}$, where g is acceleration due to gravity and H is the depth of the sea [4]. For example, if the sea depth is about 5 km then the tsunami wave velocity is about 800 km/hr. Since the wavelength of tsunami is much larger than the depth of ocean, it is characterized by as shallow water waves. A tsunami can have a period in the range of 10 minutes to 2 hours and wavelengths greater than 500 km. Therefore, we can use shallow water equations (SWE) to predict surge levels along the coast line due to tsunami. The rate at which a wave loses its energy is inversely proportional to the wavelength [5]. This is due to the fact that the velocity is proportional to the wavelength of a wave in a dispersive medium. Thus, the wave of larger wavelength reaches the shore with larger velocity and shows a higher run-up and it causes more destruction in comparison to the wave of smaller wavelength.

It is well-known that a tsunami gains height due to ‘shoaling’ effect on the coastal basin. If the trough of a tsunami reaches the coast first then it causes a phenomenon called drawdown, where it appears that sea level has dropped considerably. Drawdown is followed immediately by the crest of the wave. When the crest of the wave hits, sea level rises that is called run-up. Run-up is usually expressed in meters above normal high tide. Run-ups from the same tsunami can vary because of the influence of coastal basin i.e. the bathymetry of the coastal basin. There are a lot of studies of run-up for linear bathymetry [6, 7, 8, 9, 10, 11, 12, 13, 14, 15] only. However, the topography/bathymetry for each basin is different. The purpose of this paper is to investigate qualitatively how the run-ups of tsunami vary according to the variation of bathymetry. In section 2, we derive the differential equation required for this investigation from the conservation laws of mass and momentum of Euler [16]. For this purpose, we find that the shallow water equations (SWE) are useful. For simplicity, one-dimensional model is considered. In section 3, we present the models of various bathymetries and find the solutions of the differential equations. The numerical results obtained for the cases are plotted graphically. Finally, we make some concluding remarks in section 4.

II. DERIVATION OF DIFFERENTIAL EQUATION AND ITS SOLUTION

The shallow water equations (SWE) are a system of hyperbolic partial differential equations governing the flow of fluid in the rivers, channels, oceans and coastal regions. We have investigated SWE from mass and momentum conservation principles expressed in Navier-Stokes equations. SWE give the idea about the flow of water waves whose wavelength is much larger than depth of water. One can get SWE by neglecting bottom friction and assuming long wave approximations from the Euler equations of mass and momentum [16]. The SWE in one-dimension are given by

$$\frac{\partial \eta}{\partial t}+\frac{\partial M}{\partial x}=0, \tag{1}$$

and

$$\frac{\partial M}{\partial t}+gD\frac{\partial \eta}{\partial x}=0. \tag{2}$$

where η is water surface elevation, M is discharge flux in the negative x-axis (water is flowing along negative x-axis), g is the acceleration due to gravity, D is total thickness of water, H is the basin depth of water ($D=\eta+H$) .

As the wave reaches the coastal region, the depth of basin begins to decrease. Then, $D=\eta+h$, where $h=h(x)$. In this region, we can get a single uncoupled equation from (1) and (2). By partial differentiation with respect to t of (1) and that with respect to x of (2) and taking difference and neglecting the nonlinear terms, we get

$$\frac{\partial^2 \eta}{\partial t^2}-g\frac{\partial}{\partial x}\left(h\frac{\partial \eta}{\partial x}\right)=0. \tag{3}$$

With the help of (3), we shall try to analyze the run-up of tsunami in the coastal region for various forms of coastal basin. We consider that the basin lies in the fourth quadrant of the co-ordinate system such that the depth is in the negative y-axis and water surface is in the positive x-axis.

The origin is taken as the point where still water touches the coast. We shall first consider $h(x)=-\alpha x^n$, where n is a parameter which determines the shape of a bathymetry and α is also a parameter which determines the steepness of the bathymetry for a particular n. It is to be mentioned that the incident wave suffers negative geometry of the bathymetry. In particular, the depth of the ocean increases from the shore (x=0) to the higher x values but as the wave moves towards the shore the depth of the basin decreases. Thus we should put $h(x)=\alpha x^n$ in (3) to derive the required differential equation. The wave height η is a function of both x and t. For separation of variables, we consider

$$\eta(x,t)=u(x)v(t), \tag{4}$$

and

$$v(t)=a\sin\omega t, \tag{5}$$

where a is the amplitude and ω is the angular frequency of the wave. Putting (4) and (5) and $h(x)=\alpha x^n$ in (3), we have the linear second order differential equation as

$$xu''(x)+nu'(x)+\frac{\omega^2}{g\alpha x^{n-1}}u(x)=0. \tag{6}$$

The general solution of (6) is given by

$$u(x)=m^p\left(\sqrt{x}\right)^{1-n}\begin{Bmatrix} J_p\left(\frac{2(\sqrt{x})^{2-n}}{m}\right)C_1\Gamma\left(\frac{1}{2-n}\right)+ \\ J_{-p}\left(\frac{2(\sqrt{x})^{2-n}}{m}\right)C_2\Gamma\left(\frac{2n-3}{2-n}\right)\end{Bmatrix}, \tag{7}$$

where $m=\frac{\sqrt{g\alpha}(2-n)}{\omega}$, $p=\frac{1-n}{n-2}$, C_1 and C_2 arbitrary constants, J represents the Bessel function of the first kind and Γ denotes the gamma function. For $n<1$, p is negative and for $n>1$, p is positive. First, we shall discuss about the wave form of $u(x)$ with the variation of n for particular values of ω and α. Secondly, we shall discuss the forms of $u(x)$ for different values of α and ω for some particular value of n.

III. MODELS OF BATHYMETRY AND RUN-UP

A. Variation of *n* with constant *α*

The forms of bathymetries, $h(x)=-\alpha x^n$, for particular values of α, α=0.2 (say), for three different values of n are shown in Figure 1. In this figure we see the forms of basin bathymetries for n=0.4, 1 and 1.8. The curves for n<1 are concave in nature and those for n>1 are convex. It is evident that the bathymetry is a straight line for n=1.

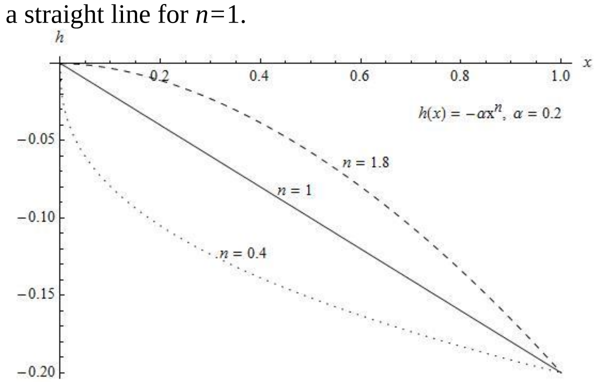

FIGURE 1. Forms of basin bathymetry for different values of n. The dotted curve is for n=0.4 (concave), solid line is for n=1 (linear) and the dashed curve is for n=1.8 (convex).

To get the numerical results we further consider that the values of the constants C_1 and C_2 are 1 in (7). We find the solutions, $u(x)$ for n=0.4, 0.6, 0.8, 1, 1.2 and 1.4 as given below.

$$u(x)_{0.4}=0.83804x^{0.3}\left(\frac{\omega}{\sqrt{(g\alpha)}}\right)^{\frac{3}{8}}\times \left[1.43452J_{-\frac{3}{8}}\left(1.25x^{0.8}\frac{\omega}{\sqrt{(g\alpha)}}\right)+ 0.888914J_{\frac{3}{8}}\left(1.25x^{0.8}\frac{\omega}{\sqrt{(g\alpha)}}\right)\right], \tag{8}$$

$$u(x)_{0.6} = 0.90834x^{0.2}\left(\frac{\omega}{\sqrt{(g\alpha)}}\right)^{\frac{2}{7}} \times$$
$$[1.27599J_{-\frac{2}{7}}\left(1.42857x^{0.7}\frac{\omega}{\sqrt{(g\alpha)}}\right) +$$
$$0.89975J_{\frac{2}{7}}\left(1.42857x^{0.7}\frac{\omega}{\sqrt{(g\alpha)}}\right)], \quad (9)$$

$$u(x)_{0.8} = 0.97007x^{0.1}\left(\frac{\omega}{\sqrt{(g\alpha)}}\right)^{\frac{1}{6}} \times$$
$$[1.12879J_{-\frac{1}{6}}\left(\frac{1}{6}x^{0.6}\frac{\omega}{\sqrt{(g\alpha)}}\right) + 0.927719J_{\frac{1}{6}}\left(\frac{1}{6}x^{0.6}\frac{\omega}{\sqrt{(g\alpha)}}\right)] , \quad (10)$$

$$u(x)_1 = 2J_0\left(2\sqrt{\left(\frac{x\omega}{g\alpha}\right)}\right), \quad (11)$$

$$u(x)_{1.2} = 0.94574x^{-0.1}\left(\frac{\omega}{\sqrt{(g\alpha)}}\right)^{-\frac{1}{4}} \times$$
$$[1.22542J_{-\frac{1}{4}}\left(2.5x^{0.4}\frac{\omega}{\sqrt{(g\alpha)}}\right) +$$
$$0.906402J_{\frac{1}{4}}\left(2.5x^{0.4}\frac{\omega}{\sqrt{(g\alpha)}}\right)], \quad (12)$$

and

$$u(x)_{1.4} = 0.711379x^{-0.2}\left(\frac{\omega}{\sqrt{(g\alpha)}}\right)^{-\frac{1}{3}} \times$$
$$[2.67894J_{-\frac{2}{3}}\left(\frac{10}{3}x^{0.3}\frac{\omega}{\sqrt{(g\alpha)}}\right) + 0.902745J_{\frac{2}{3}}\left(\frac{10}{3}x^{0.3}\frac{\omega}{\sqrt{(g\alpha)}}\right)]. \quad (13)$$

We plot the $u(x)$'s against x as obtained in equations (8 – 10) in Figure 2 to get an idea about the behavior of tsunami near the shore when the concavity of the bathymetry gradually decreases. The solid, dotted and dashed curves represent the n values for 0.4, 0.6 and 0.8 respectively. The numbers for these curves have been obtained by putting g=10, α=0.2 and ω=π/10.

From Figure 2, it is clear that as n increases the amplitude (run-up) of tsunami near the coastal line increases. All the curves have the numerical value u=1 at x=0 for our assumption that the constants (C_1 and C_2) have values equal to 1. But at x≈2.5, the values of u are 1.2, 1.3 and 1.5 for n=0.4, 0.6 and 0.8 respectively. We have checked that the results are consistent for any intermediate value of n. In view of this, we can say that as the concavity decreases i.e. the bathymetry changes its shape from concave to straight line the run-up of tsunami increases. If we look closely into the curves we see that the more concave the bathymetry (lower value of n) represents the smaller value of wavelength of tsunami.

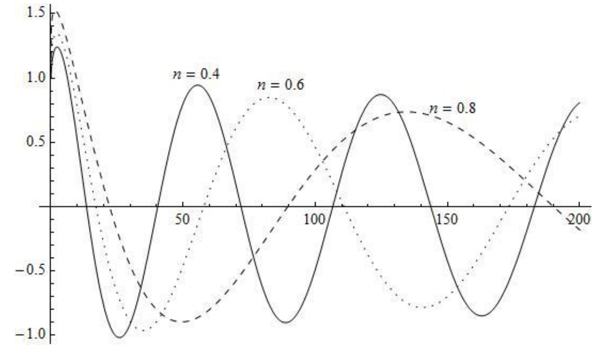

FIGURE 2. Plot of *u(x)* vs. *x* for different values of *n*. The solid curve is for *n*=0.4, dotted curve for *n*=0.6 and dashed curve for *n*=0.8.

Here the wavelength is minimum for n=0.4 and maximum for n=0.8. It is known to us that the wave of higher wavelength carries more velocity (energy) and thus attacks at the shore with higher energy.

Now, we will see the effect of tsunami when the bathymetry changes the shape from linear to convex i.e. for $n \geq 1$. Thus we plot (11 – 13) in Figure 3. The solid curve represents the incoming wave for n=1 (linear bathymetry), the dotted curve for n=1.2 and the dashed curve for n=1.4. If we look closely into the curves, we see that the wavelength is the largest for n=1.4 and the smallest for n=1. In particular, the wave for higher n value is more violent than the wave of lower n value. Thus we can say that the bathymetry for higher n value causes not only greater run-up but also more inundation in the coastal region. Thus our result is consistent when the bathymetry changes its shape from concave to convex.

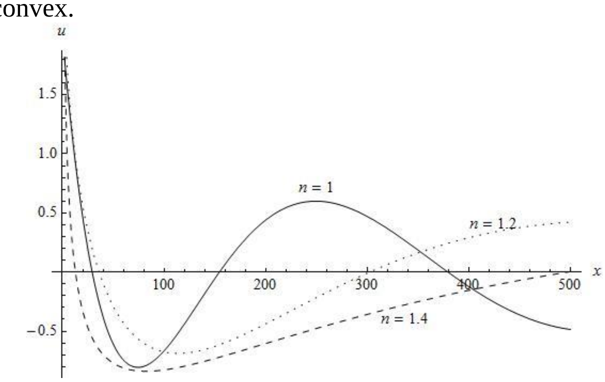

FIGURE 3: Plot of *u(x)* vs. *x* for different values of *n*. The solid curve is for *n*=1, dotted curve for *n*=1.2 and dashed curve for *n*=1.4.

B. Variation of *α* for constant value of *n*

Now, we shall discuss the effect of α for a particular value of n in the run-up of tsunami. For simplicity, we take n=1. Thus the depth of the basin follows the equation h=- αx. The basin bathymetry for different values of α will have the form as shown in Fig. 4. In this figure we have drawn $h(x)$ for α=0.2 and 0.4. As α increases the steepness of the basin increases.

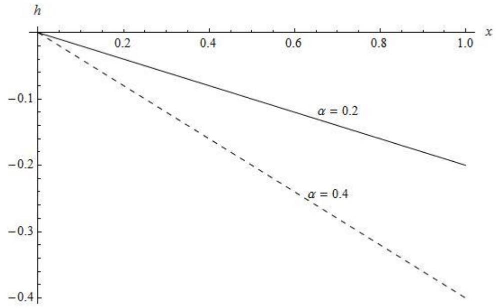

FIGURE 4. Graphical representation of the linear bathymetry following the equation *h(x)=-αx* for two different values of *α* (*α*=0.2 (solid line) and *α*=0.4 (dashed line)).

From each of the wave equations given in (8 – 13), it is clear that the run-up of tsunami not only depends upon *α* but also on the angular frequency *ω* of the wave. The wave form for *n*=1 can be taken as

$$u(x) = J_0\left(2\sqrt{\left(\frac{x\omega}{g\alpha}\right)}\right) = J_0\left(\sqrt{\left(\frac{2}{5}\right)}\sqrt{\left(\frac{\omega x}{\alpha}\right)}\right) \tag{14}$$

where the multiplicative factor 2 in front of (11) is not considered and putting *g*=10. We choose two values of *α* and *ω* each for showing the dependence of *u*(*x*) on them. In particular, we plot *u*(*x*) for *α*=0.2 and 0.4 for two different values of *ω*, viz. *ω*=*π*/10 and *π*/20. The expressions are given by

$$u_1(x) = J_0(0.444288\sqrt{x}), \tag{15}$$

for $\omega = \pi/10$ and $\alpha = 0.2$,

$$u_2(x) = J_0(0.314159\sqrt{x}), \tag{16}$$

for $\omega = \pi/10$ and $\alpha = 0.4$,

$$u_3(x) = J_0(0.222144\sqrt{x}), \tag{17}$$

for $\omega = \pi/20$ and $\alpha = 0.2$ and

$$u_4(x) = J_0(0.15708\sqrt{x}), \tag{18}$$

for $\omega = \pi/20$ and $\alpha = 0.4$.

Figure 5 shows the variations of *u*(*x*)'s with *x* given in (15 – 18). As the Bessel function of zero order is equal to 1 at *x*=0, thus all the equations bear equal value (1) at this point. Here (*a*) (solid line) and (*b*) (dashed line) show the variations of *u*(*x*) for *α*=0.2 and 0.4 respectively when *ω*=*π*/10 whereas (*c*) (dot-dashed line) and (*d*) (dotted line) give the results for *α*=0.2 and 0.4 when *ω*=*π*/20. Comparing (*a*) and (*b*) or (*c*) and (*d*) we can say that for fixed value of *ω*, the oscillatory behavior of *u*(*x*) decreases for increasing value of *α*. In other words, the troughs/crests of the wave are observed at larger distances for higher *α*. More specifically, the wavelength increases with *α* for fixed *ω*. Thus more is the steepness of the bathymetry higher is the run-up which agrees with [15]. Similarly, by comparing the graphs of (*a*) and (*c*) or (*b*) and (*d*) we can draw the inference about the effect of *ω* for a particular value of *α*. In both of the cases we see that the wavelength increases with decreasing *ω*.

This is in agreement with [14] which describes that the waves which come later (lower frequency) are more violent than the waves with higher frequency. Actually, the distance between two consecutive peaks depends upon the argument of the Bessel function. If both *α* and ω change then we have to consider the value of *ω*/√*α*. The wavelength of *u*(*x*) increases with decreasing value of *ω*/√*α*. We know that the rate of loss of energy of a wave is inversely proportional to its wavelength. In the above four cases, the energy loss will be minimum for (*d*) and it increases gradually from (*d*) to (*a*). Thus the higher values of *α* and lower values of *ω* show larger run-up and hence affect the shore more violently during tsunami. This is true for any other value of *n*.

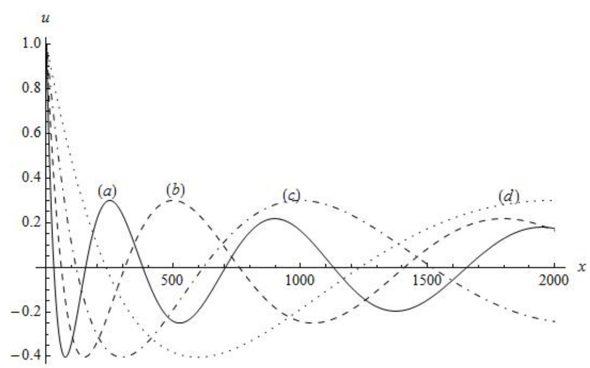

FIGURE 5. Variation of *u(x)* with *x;* (*a)* and (*b*) for *α*=0.2 and *α*=0.4 when *ω*=*π*/10, (*c*) and (*d*) for *α*=0.2 and *α*=0.4 when *ω*=*π*/20.

IV. CONCLUSION

We derived a linear partial differential equation to explain the run-up of tsunami in different bathymetry of the coastal basin. The solution of the equation is obtained in analytic form. It is used to demonstrate how the run-up of tsunami changes as the basin topography changes from concave to convex including the linear form. Our study clearly shows that the run-up of tsunami increases gradually as the bathymetry goes from concave to convex. This is physically realizable because more is the convexity of the coastal basin larger will be the opposing factor to face the tsunami. This, in turn, helps accumulate greater amount of water of the incoming wave. We have also explained how the run-up depends on the steepness of the basin. For a particular bathymetry of fixed *n* and for a fixed frequency of incoming wave, the run-up of tsunami also increases with steepness parameter α which, in other words, satisfies the observation in [15]. In this context we have got that less is the frequency of the tsunami larger run-up is observed which is in agreement with [14].

REFERENCES

[1] Titov, V., Rabinovich, A., Mofjeld, H., Thomson, R. and González, F., *The global reach of the 26 December 2004 Sumatra tsunami*, Science **309**, 2045 (2005).

[2] Dias, F., Dutykh, D., O'Brien L., Renzi E. and Stefanakis, T., *On the Modelling of Tsunami Generation and Tsunami Inundation*, Procedia IUTAM **10**, 338 (2014).

[3] Imamura, F. and Yalcine, A. C., *Tsunami Modeling Manual (Draft)*, (2006) pp. 1 - 58.

[4] Martin, P. A., Dalrymple, R. A. and Kirby, J. T., *Gravity Waves in Water of Finite Depth* Chapter 5, (Computational Mechanics Publications, Southampton, 1997), pp. 169 – 213.

[5] Gisler, G., Weaver, R. and Gittings, M. L., *Sage calculations of the tsunami threat from La Palma*, Science of Tsunami Hazards **24**, 288 (2006).

[6] Carrier, G. and Greenspan, H., *Water waves of finite amplitude on a sloping beach*, J. Fluid Mech. **4**, 97 (1958).

[7] Synolakis, C. E., *The runup of solitary waves*, J. Fluid Mech **185**, 523 (1987).

[8] Tadepalli, S. and Synolakis, C. E., *The run-up of N-waves on sloping beaches*, Proc. R. Soc. Lond. A. **445**, 99 (1994).

[9] Brocchini, M. and Peregrine, D. H., *Integral flow properties of the swash zone and averaging*, J. Fluid Mech. **317**, 241 (1996).

[10] Kânoğlu, U. and Synolakis, C., *Initial Value Problem Solution of Nonlinear Shallow Water-Wave Equations*, Phys. Rev. Lett. **97**, 148501 (2006).

[11] Didenkulova, I. I, and Pelinovsky, E. N., *Run-up of long waves on a beach: The influence of the incident wave form*, Oceanology **48**, 1 (2008).

[13] Antuono, M. and Brocchini, M., *Solving the nonlinear shallow-water equations in physical space*, J. Fluid Mech. **643**, 207 (2010).

[14] Stefanakis, T., Dias, F. and Dutykh, D., *Local Run-Up Amplification by Resonant Wave Interactions*, Phys. Rev. Lett. **107**, 124502 (2011).

[15] Stefanakis, T., Xu, S., Dutykh, D. and Dias, F., *Run-up amplification of transient long waves*, Appl. Math. **73**, 177 (2015).

[16] Vreugdenhil, C. B., *Numerical Methods for Shallow Water Flow*, (Kluwer Academic Publishers, Boston, 1994).